

Electronic Supplementary Information

Table S1. Different AOPs for degradation of glyphosate in water

AOPs	Catalyst	Reaction conditions	Remark	Reference
Activated catalyst (AC)	$\text{Co}_3\text{O}_4/\text{g-C}_3\text{N}_4$	Gly: 50 mg/L Catalyst: 50 mg/L PMS: 200 mg/L pH 11	94.28 % after 10 min Main active species: $\text{O}_2^{\bullet-}$; ${}^1\text{O}_2$ After five cycles: 83.56%	This work
Activated catalyst (AC)	$\text{Fe}_3\text{Ce}_1\text{O}_x$	Gly: 100 mg/L Catalyst: 3 g/L PMS: 154 mg/L pH 3	100% after 16 min Main active species: $\text{SO}_4^{\bullet-}$ and HO^{\bullet}	[1]
Activated catalyst (AC)	Cu^{2+}	Gly: 6 μM Catalyst: 0.025 mM Sulfite: 0.25 mM pH 9	71% after 5 min Main active species: $\text{SO}_4^{\bullet-}$ and HO^{\bullet}	[2]
Electro-Fenton (EF)	Fe^{2+}	Anode: $\text{RuO}_2/\text{IrO}_2$ Cathode: activated carbon fibers Applied current intensity: 0.36 A/cm ² O_2 flow rate: 100 mL/min Catalyst: 5.6 mg/L Gly: 17 mg/L pH 3	85% of after 120 min	[3]
Electro-Fenton (EF)	Fe^{2+}	Anode: $\text{TiO}_2/\text{PbO}_2$ Cathode: Carbon felt Applied current intensity: 10mA/cm ² Catalyst: 2.8 mg/L Gly: 17 mg/L Na_2SO_4 : 0.05 M pH 3	91.91% after 40 min. Main active species: HO^{\bullet}	[4]

Catalytic wet air oxidation (cWAO)	Fe-CNF/ ACB	Gly: 100 mg/L Catalyst: 750 mg/L pH 8.6 Temperature: 220 °C Pressure: 25 bar	70% after 2 h Main active species: HO•	[5]
Catalytic wet air oxidation (cWAO)	MWCNT-Al	Gly: 100 mg/L Catalyst: 8 g/L H ₂ O ₂ : 947 mg/L pH 5 Oxygen gas flow rate: 400 mL/min pH 9	31.5% after 2 h	[6]
Photocatalyst (PC)	10%CoS/BiOBr	Gly: 17 mg/L Catalyst: 400 mg/L Lamp: LED (40W)	74.7% after 180 min Main active species: electrons and holes	[7]
Photocatalyst (PC)	1%Cu ₂ S/Bi ₂ WO ₆	Gly: 17 mg/L Catalyst: 400 mg/L Lamp: LED (44 W)	73.2% after 180 min Main active species: h ⁺ , e ⁻ , and O ₂ •	[8]

References:

- [1] L. Xue, L. Hao, H. Ding, R. Liu, D. Zhao, J. Fu, M. Zhang, Complete and rapid degradation of glyphosate with Fe₃Ce₁O_x catalyst for peroxyomonosulfate activation at room temperature, Environ. Res. 201 (2021) 111618.
- [2] L. Chen, X. Huang, M. Tang, D. Zhou, F. Wu, Rapid dephosphorylation of glyphosate by Cu-catalyzed sulfite oxidation involving sulfate and hydroxyl radicals, Environ. Chem. Lett. 16 (2018) 1507-1511.
- [3] H. Lan, W. He, A. Wang, R. Liu, H. Liu, J. Qu, C.P. Huang, An activated carbon fiber cathode for the degradation of glyphosate in aqueous solutions by the Electro-Fenton mode: Optimal operational conditions and the deposition of iron on cathode on electrode reusability, Water Res. 105 (2016) 575-582.
- [4] M.H. Tran, H.C. Nguyen, T.S. Le, V.A.D. Dang, T.H. Cao, C.K. Le, T.-D. Dang, Degradation of glyphosate herbicide by an electro-Fenton process using carbon felt cathode, Environ. Technol. 42 (2021) 1155-1164.
- [5] P. Gupta, K. Pandey, N. Verma, Augmented complete mineralization of glyphosate in wastewater via microbial degradation post CWAO over supported Fe-CNF, Chem. Eng. J. 428 (2022) 132008.
- [6] N. Tan, Z. Yang, X.-b. Gong, Z.-r. Wang, T. Fu, Y. Liu, In situ generation of H₂O₂ using MWCNT-Al/O₂ system and possible application for glyphosate degradation, Sci. Total Environ. 650 (2019) 2567-2576.
- [7] Q.-Y. Tang, M.-J. Yang, S.-Y. Yang, Y.-H. Xu, Enhanced photocatalytic degradation of glyphosate over 2D CoS/BiOBr heterojunctions under visible light irradiation, J. Hazard. Mater. 407 (2021) 124798.
- [8] Q.-Y. Tang, W.-F. Chen, Y.-R. Lv, S.-Y. Yang, Y.-H. Xu, Z-scheme hierarchical Cu₂S/Bi₂WO₆ composites for improved photocatalytic activity of glyphosate degradation under visible light irradiation, Sep. Purif. Technol. 236 (2020) 116243.

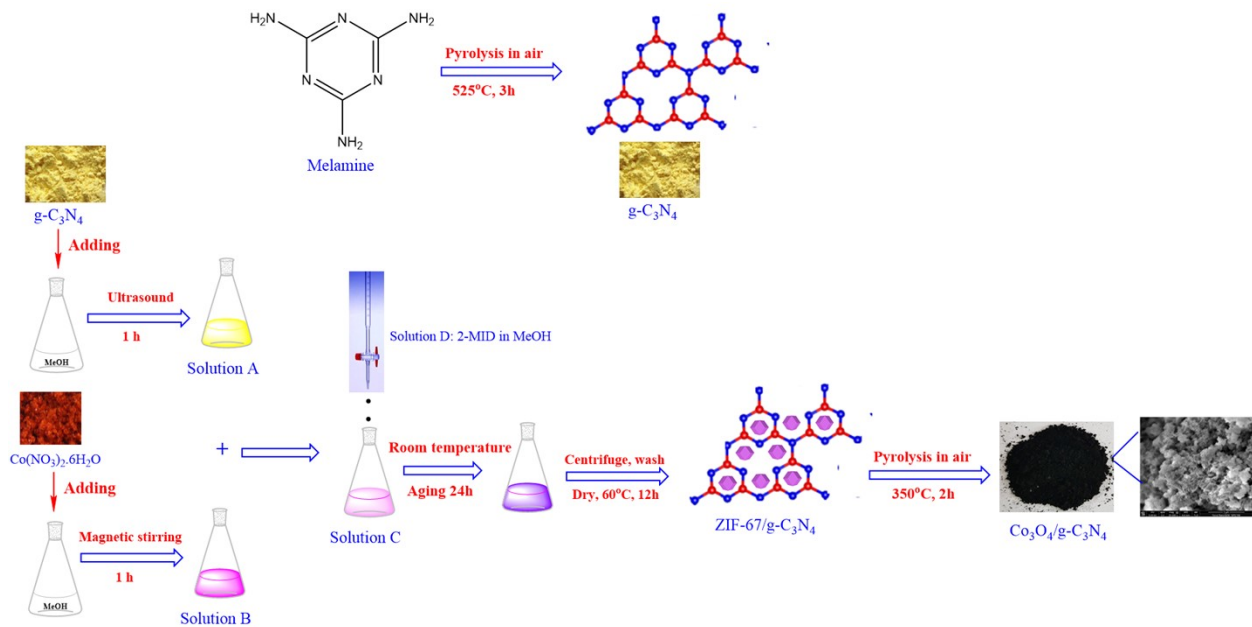


Figure S1. Procedure for the synthesis of $\text{Co}_3\text{O}_4/\text{g-C}_3\text{N}_4$ composite

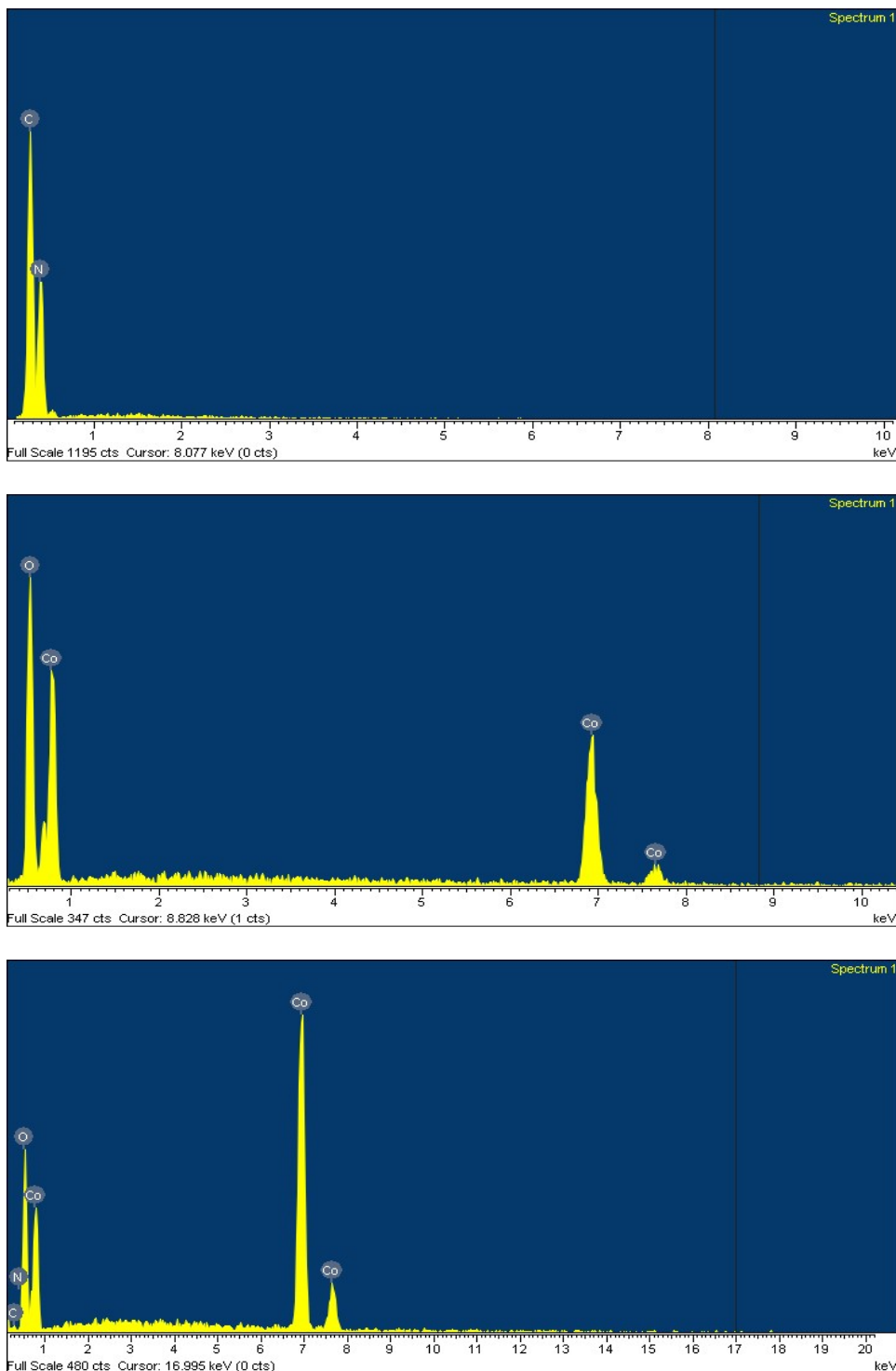


Figure S2. EDX results of (a) g-C₃N₄, (b) Co₃O₄, and (c) Co₃O₄/g-C₃N₄ materials

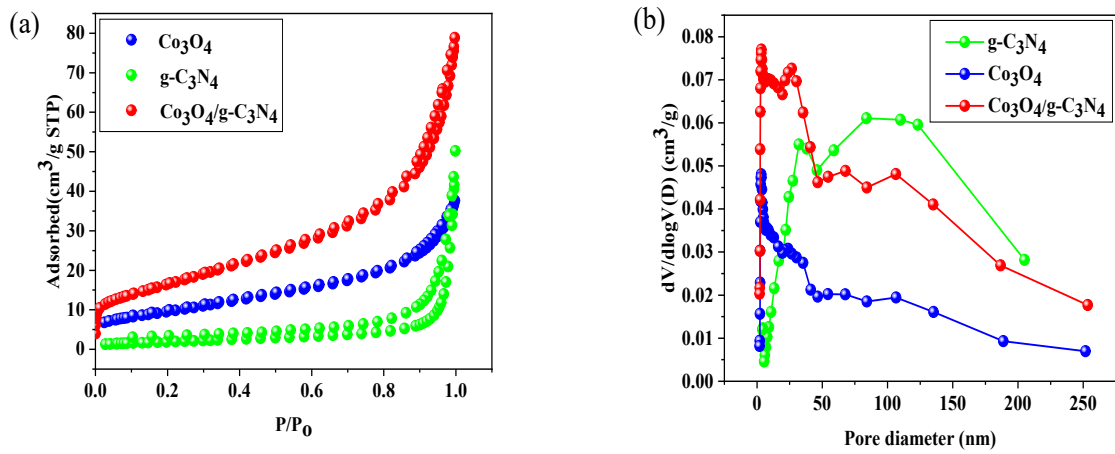


Figure S3. (a) N_2 adsorption and desorption isotherms and (b) pore size distributions of Co_3O_4 , $\text{g-C}_3\text{N}_4$, and $\text{Co}_3\text{O}_4/\text{g-C}_3\text{N}_4$ (10%)

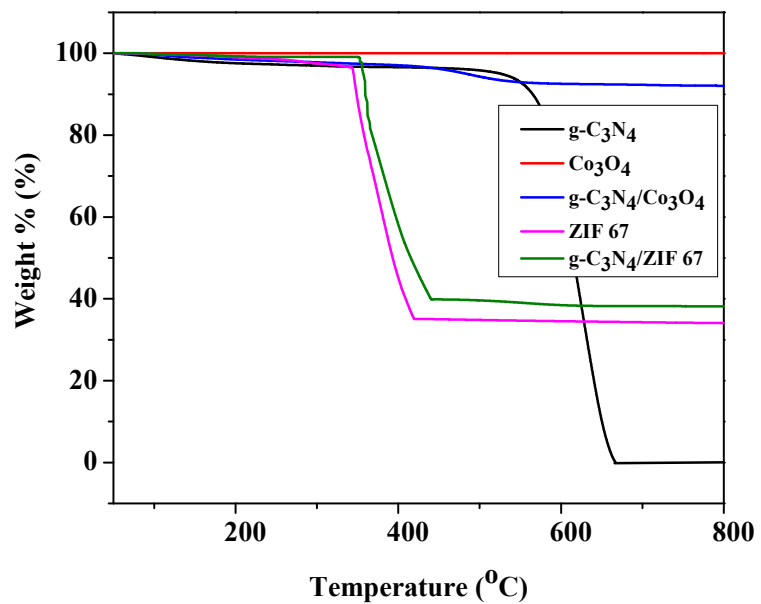


Figure S4. TGA curves of g-C₃N₄, ZIF-67, g-C₃N₄/ZIF-67, Co₃O₄, and Co₃O₄/g-C₃N₄

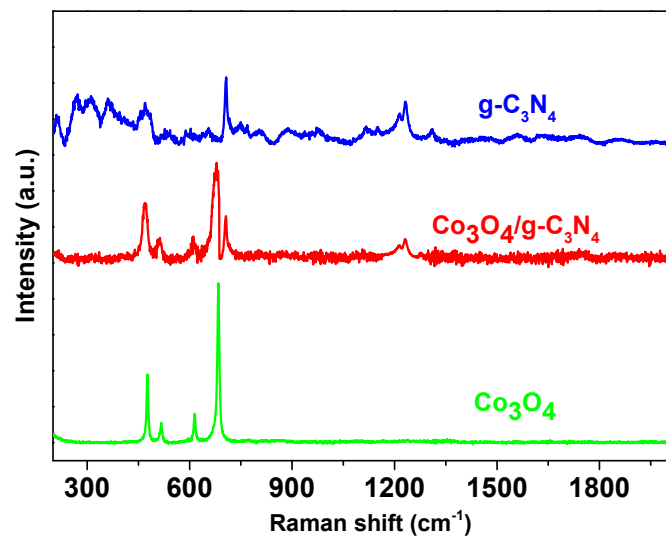


Figure S5. Raman spectra of Co₃O₄, g-C₃N₄ and Co₃O₄ /g-C₃N₄ (10%)

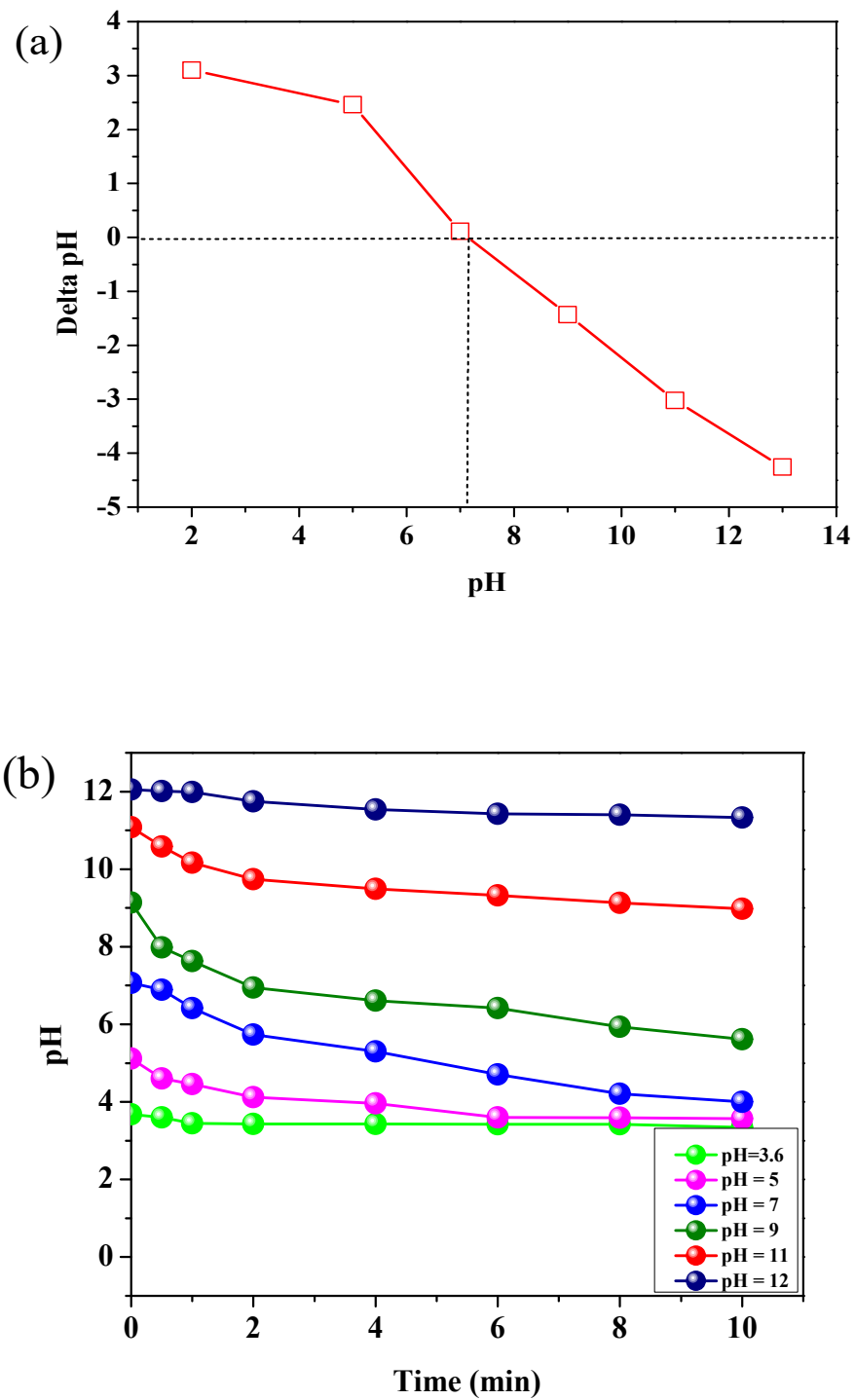


Figure S6. (a) The pH_{pzc} of $\text{Co}_3\text{O}_4/\text{g-C}_3\text{N}_4$ material and (b) the change of pH during the reaction time

(Reaction condition: 50 mgGly/L, 50 mgcatalyst/L, 200 mgPMS/L, 25 °C)

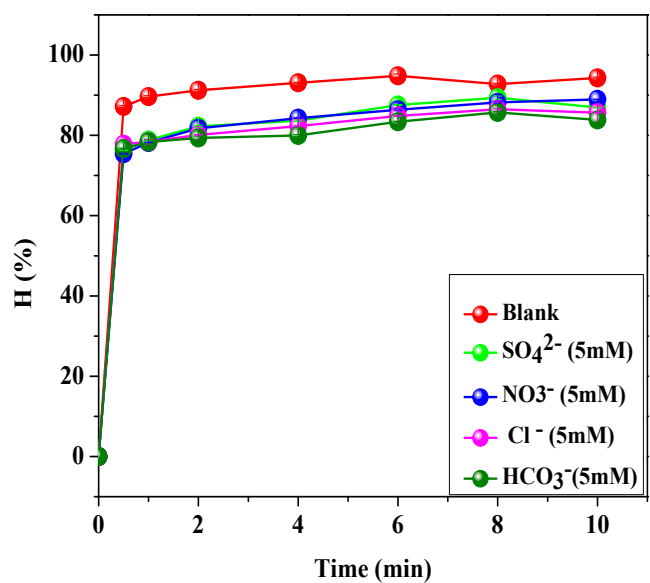


Figure S7. Effect of co-existing ions on the glyphosate decomposing at low ion concentration
(Reaction condition: 50 mgGly/L, 50 mgcatalyst/L, 200 mgPMS/L, pH 11, 25 °C)

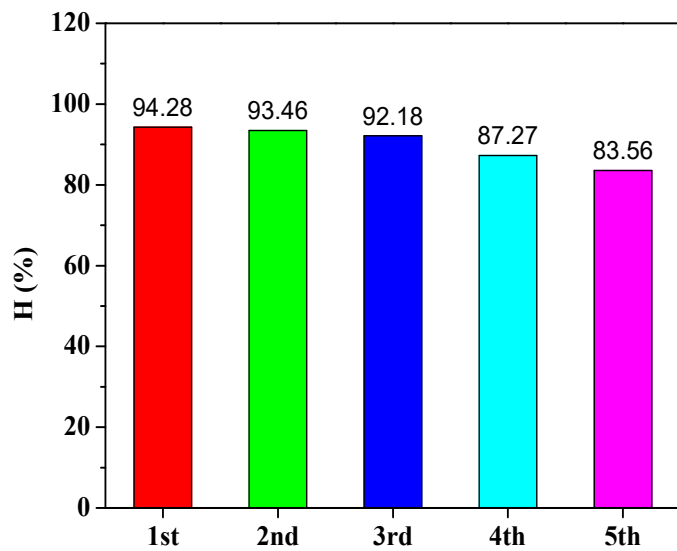


Figure S8. Glyphosate efficiency after 5 consecutive cycles of reuse
(Reaction condition: 50 mgGly/L, 50 mgcatalyst/L, 200 mgPMS/L, pH 11, 25 °C)

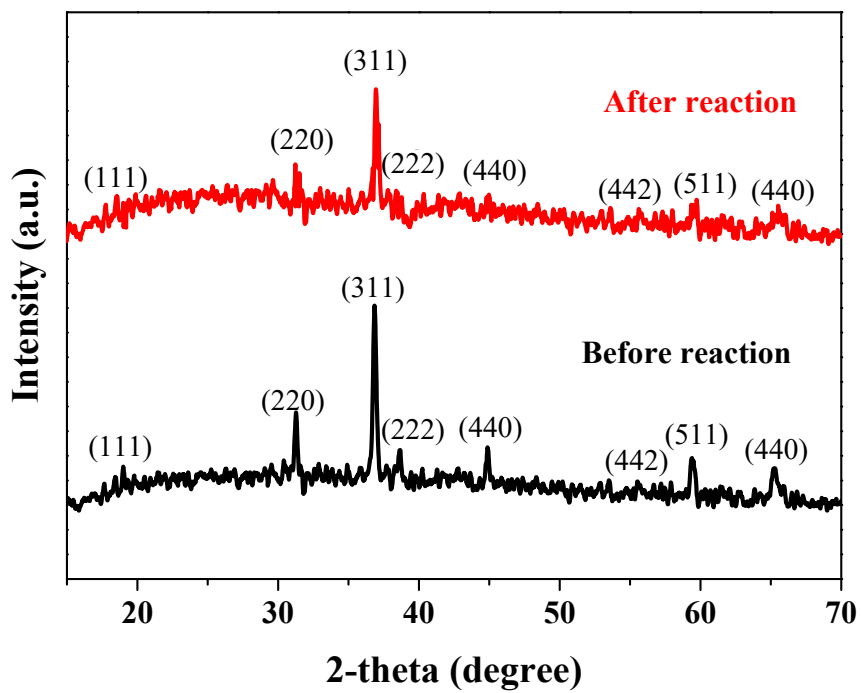


Figure S9. XRD patterns of fresh and used $\text{Co}_3\text{O}_4/\text{g-C}_3\text{N}_4$ (10%)

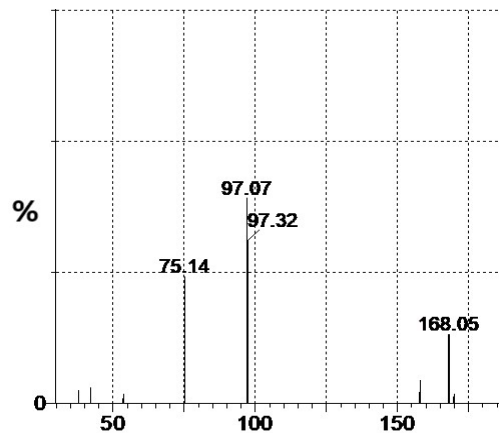


Figure S10. MS result of glyphosate solution decomposed by $\text{Co}_3\text{O}_4/\text{g-C}_3\text{N}_4/\text{PMS}$

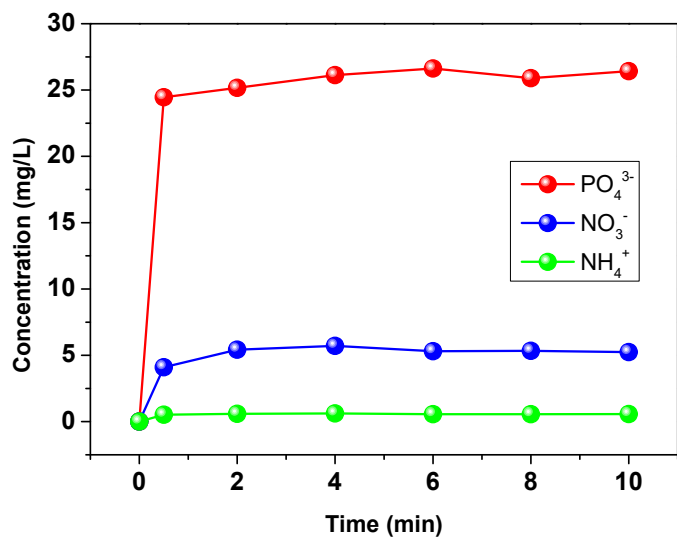


Figure S11. Concentration of ions during the glyphosate decomposition

(Reaction condition: 50 mgGly/L, 50 mgcatalyst/L, 200 mgPMS/L, pH 11, 25 °C)